

# Anion control in molecular beam epitaxy of mixed As/Sb III-V heterostructures

Brian R. Bennett,<sup>a)</sup> B. V. Shanabrook, and M. E. Twigg

*Electronics Science and Technology Division, Naval Research Laboratory, Washington, DC 20375-5347*

(Received 9 July 1998; accepted for publication 11 November 1998)

Superlattices consisting of As monolayers (MLs) in (In,Ga,Al)Sb and Sb MLs in (In,Ga,Al)As were grown by molecular beam epitaxy and characterized by x-ray diffraction, Raman spectroscopy, and high-resolution transmission electron microscopy. In all cases, well-defined superlattices were formed when the growth temperature was sufficiently low. As temperature increases for the As MLs in antimonides, substantial intermixing occurs. For Sb MLs in arsenides, Sb evaporation from the surface increases with increasing growth temperature. These results are discussed in the context of device heterostructures containing InAs/GaSb and InAs/AlSb heterojunctions.

[S0021-8979(99)05104-X]

## I. INTRODUCTION

In recent years, the emergence of several potential device applications has resulted in attention to semiconductor heterostructures containing both arsenides and antimonides. Much of the work focuses on GaSb, AlSb, InAs, and related ternaries such as InGaSb because they are nearly lattice matched, with  $a_0 \approx 6.1 \text{ \AA}$ . The flexibility in device design in  $6.1 \text{ \AA}$  heterostructures is based upon the wide range of available band alignments and band gaps. Device applications include long-wavelength infrared detectors,<sup>1</sup> infrared lasers,<sup>2,3</sup> high-frequency, low-voltage field-effect transistors,<sup>4,5</sup> resonant tunneling diodes,<sup>6</sup> and optical modulators.<sup>7</sup>

The heterostructures for these device applications include short period superlattices, extremely thin tunneling barriers, and two-dimensional electron gases. In each case, device performance is a strong function of the quality of the interfaces. Intermixing of the anion species can result in a diffuse interface.<sup>8-11</sup> Hence, growth techniques that allow good anion control are needed to achieve abrupt and reproducible interfaces.

In this work, we investigated intermixing in As/Sb heterostructures by characterizing a series of periodic (In,Ga,Al)-(As,Sb) structures in which every ninth monolayer of Sb was replaced by As or vice versa. If growth temperatures are sufficiently low, anion control is good in all cases. At higher temperatures, severe intermixing occurs if As layers are inserted into antimonides. In contrast, evaporation prevents formation of complete Sb monolayers in arsenide films. These results will be discussed in the context of recent reports on the influence of growth temperature on As/Sb device heterostructures.

## II. EXPERIMENTAL PROCEDURE

Samples were grown by solid-source molecular beam epitaxy (MBE) using As<sub>2</sub> or As<sub>4</sub> from a valved As cracker. Both a conventional Sb<sub>4</sub> cell as well as a Sb cracker producing Sb<sub>2</sub> were used. We applied migration-enhanced epitaxy to achieve the desired structures. For example, a growth se-

quence, repeated 40 times, was: (7 ML GaSb, 3 s Sb, 1 ML Ga, 7 s As, 1 ML Ga), nominally yielding a 40-period superlattice (SL) with 8 ML GaSb and 1 ML GaAs per period, as illustrated in Fig. 1. All SLs were grown at a rate of 0.5 ML/s on semi-insulating GaAs(001) substrates. For Sb MLs in GaAs and AlAs, GaAs buffer layers were used. For Sb MLs in InAs, a 1.0  $\mu\text{m}$  buffer layer of InAs was grown on the GaAs substrate to accommodate the 7% lattice mismatch. 1- $\mu\text{m}$ -thick buffer layers of InSb, GaSb, and AlSb were used for SLs with As MLs in InSb, GaSb, and AlSb, respectively. Growth temperatures were measured by transmission thermometry.<sup>12</sup> SLs were grown at several different temperatures for all six cases: As MLs in GaSb, AlSb, or InSb, and Sb MLs in GaAs, AlAs, or InAs. Samples were characterized by single-crystal x-ray diffraction (XRD), using a Cu  $K\alpha$  source and the (004) reflection. Selected samples were also characterized by Raman spectroscopy and cross-sectional, high-resolution transmission electron microscopy (HRTEM). Raman data were collected at room temperature in the  $Z(X,Y)\bar{Z}$  configuration where  $Z$  and  $\bar{Z}$  are the directions of the incident and scattered light, (\*,\*) denote the directions of polarization of the incident and scattered radiation, and  $X$ ,  $Y$ , and  $Z$  denote the [100], [010], and [001] crystallographic directions, respectively. Radiation from an Ar ion laser operating at 5145  $\text{\AA}$  was employed in the Raman measurements. HRTEM samples were ion milled at liquid nitrogen temperature (As MLs in GaSb) or cleaved in the [100] cross-sectional configuration (Sb MLs in GaAs).

## III. RESULTS

A total of 31 samples were grown and characterized in this study. The SL periods were calculated from the separation of XRD satellite peaks and ranged from 23 to 28  $\text{\AA}$ . The XRD data are simulated using dynamical diffraction theory. The SLs were modeled as consisting of two layers, the host and the alien. The thicknesses of the two layers were adjusted until the simulated data matched the experimental period and  $n=0$  satellite position ( $2\theta$ ).

XRD data for the case of As<sub>2</sub> MLs in GaSb are shown in Fig. 2. Growth temperatures of 400 and 420  $^\circ\text{C}$  produced

<sup>a)</sup>Electronic mail: brian.bennett@nrl.navy.mil

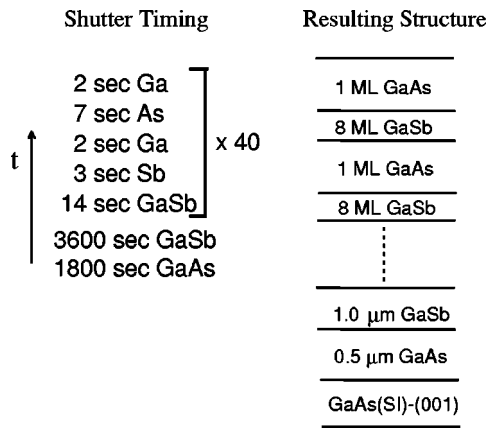


FIG. 1. Growth sequence and nominal structure for arsenic monolayers in GaSb.

structures with four satellite x-ray peaks, indicating a well-defined SL was present. (The presence of SL satellites does not prove that the As is confined to a single ML.) The SL periods are 25.6 Å (400 °C sample) and 26.6 Å (420 °C sample). The average lattice constants of the structures perpendicular to the growth direction are 5.996 Å (400 °C sample) and 5.972 Å (420 °C sample). These values are consistent with coherently strained SLs,  $1.0 \pm 0.2$  MLs GaAs per period, and  $7.6 \pm 0.2$  MLs GaSb per period. At a growth temperature of 450 °C, the  $n=0$  and  $n=-1$  satellites are present but substantially broader than at lower temperatures. For higher temperatures (480 and 520 °C), no satellites are observed. An additional sample was grown at 480 °C using As<sub>4</sub> instead of As<sub>2</sub>. The x-ray spectrum includes  $n=0$  and  $n=-1$  SL satellites, unlike the sample grown at the same temperature using As<sub>2</sub>.

The vibrational properties of As MLs in GaSb were probed by Raman spectroscopy. Room-temperature spectra

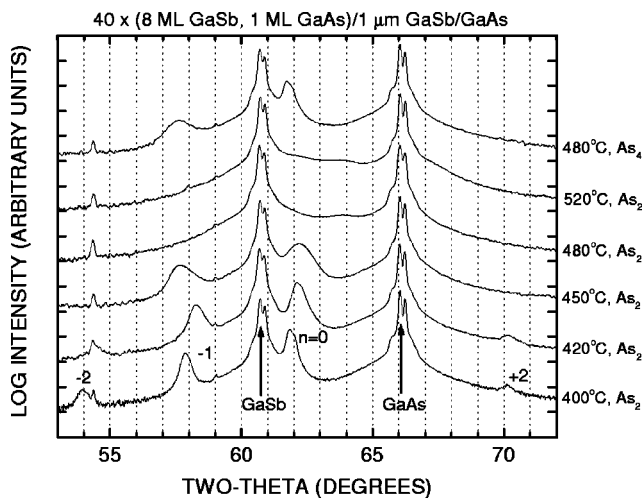


FIG. 2. X-ray diffraction  $\theta-2\theta$  scans for superlattices formed by inserting As monolayers into GaSb. The growth temperature and As species are given for each sample. In addition to the GaAs and GaSb peaks, which display  $K_{\alpha 1}-K_{\alpha 2}$  peak splitting, superlattice satellite peaks are present for the samples grown at lower temperatures. (The sharp feature near 54.3° on all scans is not a superlattice feature but is due to contamination on the x-ray tube.)

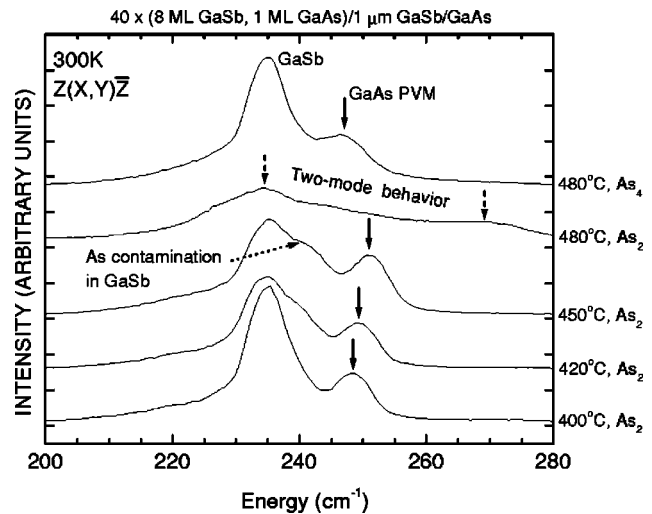


FIG. 3. Raman spectra for the samples of Fig. 2. Confined optical phonon modes for GaSb as well as GaAs planar vibrational modes (PVMs) are observed.

are shown in Fig. 3. The optical phonon modes from the GaSb layers occur near  $235 \text{ cm}^{-1}$  for all five samples. In addition, clear evidence for a GaAs-like mode localized at the As monolayer, known as a planar vibrational mode (PVM), is observed near  $250 \text{ cm}^{-1}$  for four of the samples.<sup>13</sup> At a growth temperature of 400 °C, the GaSb mode is symmetric and the GaAs PVM energy is  $248 \text{ cm}^{-1}$ . As the growth temperature is increased to 420 and 450 °C, the energy of the GaAs PVM increases slightly and additional scattering appears on the high-energy side of the GaSb peak. This scattering is probably due to enhanced As incorporation in the GaSb. At 480 °C, there is no distinct GaAs peak although additional scattering is present near  $270 \text{ cm}^{-1}$ , suggestive of two-mode behavior for GaAsSb alloys. These results are consistent with the x-ray diffraction data, which showed the SL satellites broadening at 420 and 450 °C and disappearing at 480 °C. The small increase in energy of the GaAs mode with increasing growth temperature is consistent with the As being less confined to a single monolayer as the temperature is increased.<sup>14-16</sup> The 480 °C sample with As<sub>4</sub> has a symmetric GaSb peak and a GaAs mode at an energy of  $247 \text{ cm}^{-1}$ .

Two of the GaSb:As samples were also examined by HRTEM. The SL structure was clearly observed for the sample grown at 400 °C. Image processing<sup>17</sup> indicated that the thickness of the As-containing layers was 1–2 ML. In contrast, no modulation was found for the sample grown at 480 °C with As<sub>2</sub>.

X-ray diffraction scans for two samples with As MLs (using As<sub>2</sub>) inserted into InSb are shown in Fig. 4. A well-defined SL is present for a growth temperature of 325 °C, but not at 370 °C. For As MLs in AlSb, SL satellite peaks are observed over the entire temperature range investigated, 400–580 °C, as shown in Fig. 5. Some degradation is apparent at temperatures above 500 °C.

The results are quite different for Sb MLs in (In,Ga,Al)As. For Sb<sub>4</sub> in GaAs, satellite peaks are observed from 330 to 600 °C, as shown in Fig. 6. For  $T \leq 450$  °C, the

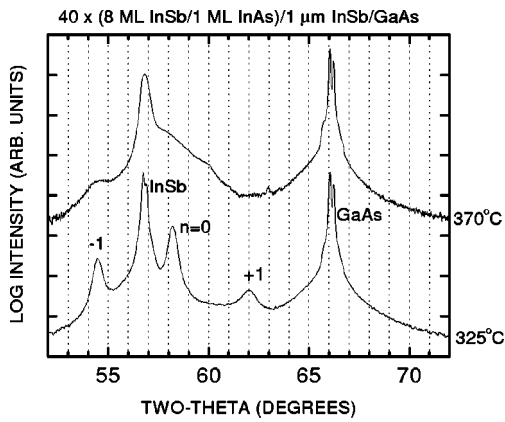


FIG. 4. X-ray diffraction  $\theta-2\theta$  scans for superlattices formed by inserting As monolayers into InSb. The  $As_2$  species was used for both samples.

average lattice constants of the structures are consistent with coherent SLs and  $1.0 \pm 0.1$  MLs GaSb per period. At higher temperatures, satellites are still present, but the amount of Sb incorporated *decreases* with increasing temperature. An additional 600 °C sample was grown using  $Sb_2$ . The results are similar to the  $Sb_4$  sample grown at the same temperature, with  $\sim 0.3$  ML Sb incorporated per period.

Samples with Sb MLs in GaAs grown at 410 and 600 °C using  $Sb_4$  were characterized by HRTEM. The corresponding images are shown in Fig. 7. As expected, modulation with a period of  $\sim 25$  Å is present in both samples but is more pronounced for the 410 °C sample. Applying an image-processing algorithm (based upon chemical lattice imaging<sup>18,19</sup>) to our HRTEM data allows us to conclude that the thickness of the Sb-containing layer is 1–2 ML for the 410 °C sample. This value is consistent with atomically abrupt interfaces and HRTEM imaging of steps that were formed during growth.<sup>17</sup> In contrast, although x-ray measurements reveal only 0.4 ML Sb per period in the 600 °C sample, analysis of HRTEM data indicates that the Sb is spread out over 4 ML, consistent with enhanced segregation at the higher growth temperature.

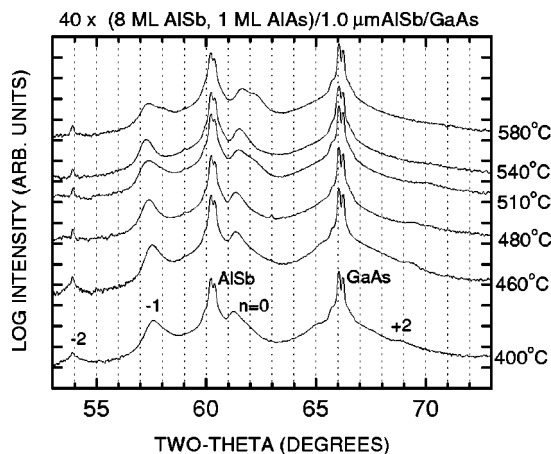


FIG. 5. X-ray diffraction  $\theta-2\theta$  scans for superlattices formed by inserting As monolayers into AlSb. The  $As_2$  species was used for all samples. (The sharp feature near 53.9° on all scans is not a superlattice feature but is due to contamination on the x-ray tube.)

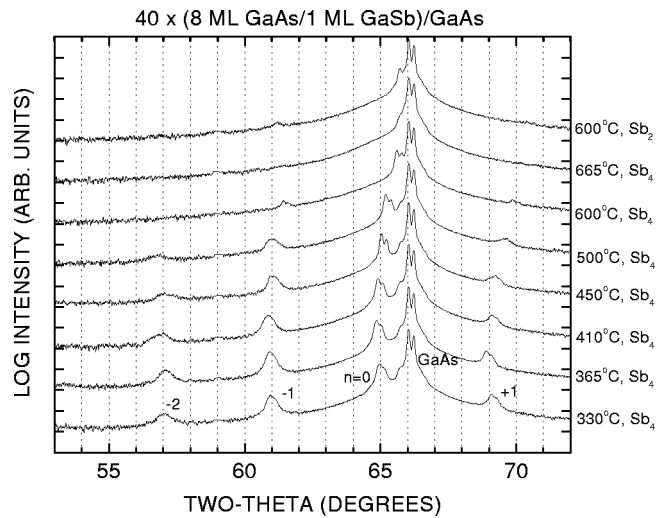


FIG. 6. X-ray diffraction  $\theta-2\theta$  scans for superlattices formed by inserting Sb monolayers into GaAs. The growth temperature and Sb species are given for each sample.

The XRD data for Sb MLs inserted into InAs are shown in Fig. 8. The results are similar to the GaAs:Sb samples. At low temperatures, approximately 1 ML of Sb is incorporated per period. As the growth temperature increases, less Sb is incorporated. For Sb MLs in AlAs (Fig. 9), only 0.8 ML Sb is incorporated per period at low temperatures, with decreasing Sb incorporation as the growth temperature increases above 480 °C.

The results for Sb MLs in (In,Ga,Al)As are summarized in Fig. 10 where we plot the number of Sb MLs incorporated per period as a function of growth temperature for all three materials; coherent SLs are assumed. We can define a critical temperature as the temperature at which the amount of Sb incorporated begins to decrease. For GaAs:Sb and AlAs:Sb, the critical temperature is approximately 470 °C, but for InAs:Sb it is near 410 °C.

IV. DISCUSSION

Yano *et al.* addressed the issue of interfacial abruptness by subjecting 1 μm layers of (In,Ga,Al)As to  $Sb_4$  beams and

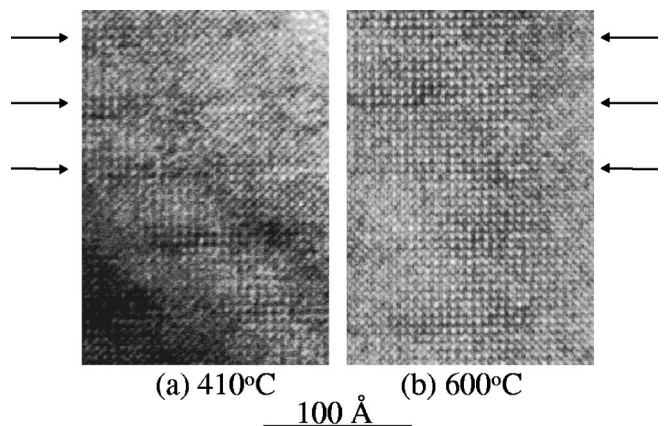


FIG. 7. HRTEM images of Sb monolayers in GaAs for growth temperatures of 410 and 600 °C. The arrows indicate the positions of the Sb.

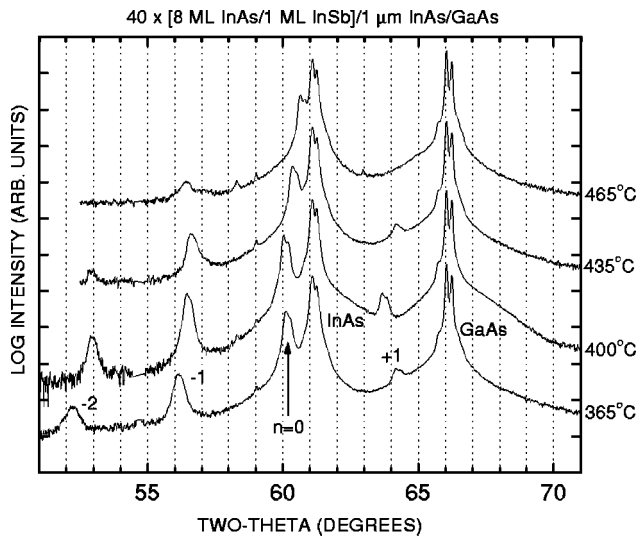


FIG. 8. X-ray diffraction  $\theta-2\theta$  scans for superlattices formed by inserting Sb monolayers into InAs. The  $\text{Sb}_4$  species was used for all samples.

(In,Ga,Al)Sb to  $\text{As}_4$  beams as a function of temperature.<sup>8</sup> They determined surface stability by examining reflection high-energy electron diffraction (RHEED) reconstructions and looking for new compounds with Raman spectroscopy. For example, a GaSb surface subjected to an  $\text{As}_4$  beam for 1800 s exhibited GaAs-like vibrational modes at temperatures above 440 °C, but was stable (i.e., only GaSb observed by Raman) at lower temperatures. The critical temperatures for the other materials were: AlSb: $\text{As}_4$ =440 °C, InSb: $\text{As}_4$ =320 °C, GaAs: $\text{Sb}_4$ =700 °C, InAs: $\text{Sb}_4$ =540 °C, and AlAs: $\text{Sb}_4$ >800 °C.

Our critical temperatures for As MLs in InSb and GaSb are in reasonable agreement with the results of Yano *et al.* At temperatures above 450 °C (350 °C) for GaSb:As (InSb:As), the As apparently intermixes with the GaSb (InSb), resulting in a GaAsSb (InAsSb) alloy. The resulting strain could lead to three-dimensional growth. This model is consistent with our observation of transmission spots in the RHEED pattern

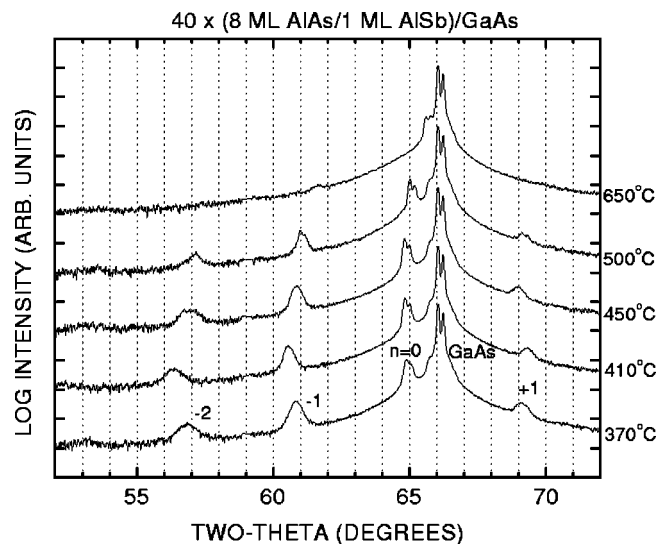


FIG. 9. X-ray diffraction  $\theta-2\theta$  scans for superlattices formed by inserting Sb monolayers into AlAs. The  $\text{Sb}_4$  species was used for all samples.

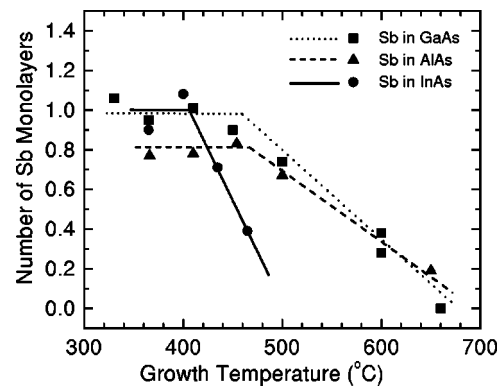


FIG. 10. Number of Sb monolayers per period as a function of growth temperature, calculated from the data in Figs. 6, 8, and 9. Lines are guides to the eye.

and the absence of a well-defined SL in x-ray diffraction or distinct GaAs planar vibrational modes in Raman spectroscopy. Our results also suggest that  $\text{As}_4$  is less aggressive than  $\text{As}_2$  in reacting with the GaSb surface. This is consistent with x-ray photoelectron spectroscopy and RHEED studies on InAs and GaSb surfaces. Wang *et al.*<sup>20</sup> and Collins *et al.*<sup>21</sup> investigated replacement of Sb on a GaSb surface during  $\text{As}_x$  irradiation. They found that  $\text{As}_2$  replaced Sb much faster than  $\text{As}_4$ . Similarly,  $\text{Sb}_2$  was more efficient than  $\text{Sb}_4$  at replacing As on an InAs surface.

For Sb MLs in GaAs, AlAs, and InAs, our results are consistent with Sb evaporation at higher temperatures. As expected, the critical temperature is lowest for InSb which also has the lowest congruent sublimation temperature (~400 °C). In contrast, the Yano *et al.* Raman measurements on arsenide layers subjected to a  $\text{Sb}_4$  flux were not affected by evaporation but were sensitive to exchange reactions and the formation of compounds such as GaSb.<sup>8</sup> Hence, their observed critical temperatures were much higher.

Our Sb in InAs results are also consistent with the thermodynamic model of Neklyudov *et al.*<sup>22</sup> They considered the formation of an InSb-like interface on GaSb and AlSb surfaces, and calculated the minimum Sb flux required to maintain an InSb surface. At fluxes typically used in MBE, a critical temperature of 390 °C was found. At higher temperatures, rapid reevaporation of Sb from the surface is expected.

The composition of mixed anion ternaries such as InAsSb is a strong function of anion fluxes, anion species, and substrate temperature. Hence, it is generally difficult to control stoichiometry. One approach is to grow digital alloy superlattices by using growth procedures similar to those used in this study. For example, to achieve 150 Å of an alloy of  $\text{InAs}_{0.8}\text{Sb}_{0.2}$ , one could grow 4 ML InAs followed by 1 ML InSb, repeated ten times. Our results (Fig. 10) show that the growth temperature should be less than 420 °C to achieve a complete ML of InSb per period; higher growth temperatures would result in an alloy with a smaller InSb mole fraction.

Heterojunctions between InAs and AlSb can, in principle, be joined by either InSb-like or AlAs-like interface bonds. Similarly, InSb- or GaAs-like interfaces are possible for InAs/GaSb heterojunctions. The ability to control interfacial composition is linked to the issues of anion intermixing and evaporation. For example, interfacial control in

InAs/GaSb can be achieved by migration-enhanced epitaxy.<sup>23</sup> To grow an InAs layer on GaSb with InSb interfaces, the growth shutter sequence is GaSb/Sb/In/InAs. For the same structure with GaAs interfaces, the sequence is GaSb/Ga/As/InAs. In the latter case, a layer of GaSb is subjected to an As beam, similar to the placement of As MLs in GaSb.

The composition of interfaces strongly affects properties in the InAs/AlSb system. Tuttle *et al.* investigated single quantum wells of InAs clad by AlSb grown by MBE at 500 °C.<sup>24</sup> They achieved high electron mobilities if and only if the lower interface was InSb-like. In earlier work, we examined InAs/AlSb SLs as a function of bond type and growth temperature, using x-ray diffraction, photoluminescence, and Raman spectroscopy as characterization tools.<sup>25,26</sup> High-quality SLs were formed with InSb bonds over the entire temperature range studied, 400–480 °C. For AlAs bonds, however, SL properties were severely degraded at the higher temperatures. In the latter case, layers of AlSb were directly exposed to an As flux. In the case of InSb bonds, however, a monolayer of In separates the As and Sb. Apparently, this monolayer reduces the Sb–As intermixing. The difference in intermixing for InSb and AlAs interfaces has also been explained in terms of the thermodynamics of interface formation.<sup>10</sup> At even higher temperatures, SLs cannot be formed with InSb bonds, as demonstrated by the Raman measurements of Yano *et al.* for samples grown at 530 °C.<sup>11</sup>

In contrast to the InAs/AlSb system, a growth temperature of 500 °C is too high for structures that include InAs/GaSb interfaces, even if InSb bonds are used. In the case of short-period InAs/(In)GaSb superlattices, Chow *et al.*<sup>27</sup> and Davis *et al.*<sup>28</sup> found that the optimal growth temperature was near 400 °C. XRD SL satellites were degraded or absent for higher temperatures. Fuchs *et al.* also found an optimal growth temperature near 400 °C for InAs/InGaSb SLs based upon photoluminescence intensity.<sup>29</sup> Yang *et al.* investigated infrared lasers consisting of superlattices of (6 ML InAs/10 ML InGaSb/6 ML InAs/14 ML AlSb). Both XRD and photoluminescence showed severe degradation for temperatures above 400 °C.<sup>30</sup> These results are consistent with our findings for As MLs in GaSb (Figs. 2 and 3). Somewhat higher growth temperatures might be possible if As<sub>4</sub> is used rather than As<sub>2</sub>.

## V. SUMMARY

In summary, we have examined superlattices consisting of As MLs in (In,Ga,Al)Sb and Sb MLs in (In,Ga,Al)As. In all cases, growth temperature is an important parameter, with well-defined SLs formed at 320–400 °C. As temperatures increase for the As MLs in antimonides, substantial intermixing occurs. For Sb MLs in arsenides, Sb evaporation from the surface increases with increasing growth temperature. These results are consistent with the growth of high-quality, InSb-bonded InAs/AlSb structures at temperatures near 500 °C. For structures in which GaSb layers are adjacent to InAs layers, however, growth temperatures must be limited to about 400 °C to prevent severe intermixing of As into the GaSb.

## ACKNOWLEDGMENTS

The authors thank A. S. Bracker, M. Fatemi, M. Goldenberg, R. J. Wagner, J. R. Waterman, and M. J. Yang for technical discussions and assistance. The Office of Naval Research supported this work.

- <sup>1</sup>F. Fuchs, U. Weimer, W. Pletschen, J. Schmitz, E. Ahlswede, M. Walther, J. Wagner, and P. Koidl, *Appl. Phys. Lett.* **71**, 3251 (1997).
- <sup>2</sup>G. W. Turner, H. K. Choi, and M. J. Manfra, *Appl. Phys. Lett.* **72**, 876 (1998).
- <sup>3</sup>W. W. Bewley, C. L. Felix, E. H. Aifer, I. Vurgaftman, L. J. Olafsen, J. R. Meyer, H. Lee, R. U. Martinelli, J. C. Connolly, A. R. Sugg, G. H. Olsen, M. J. Yang, B. R. Bennett, and B. V. Shanabrook, *Appl. Phys. Lett.* **73**, 3833 (1998).
- <sup>4</sup>X. Li, K. F. Longenbach, Y. Wang, and W. I. Wang, *IEEE Electron Device Lett.* **13**, 192 (1992).
- <sup>5</sup>J. B. Boos, B. R. Bennett, W. Kruppa, D. Park, M. J. Yang, and B. V. Shanabrook, *Electron. Lett.* **34**, 403 (1998); J. B. Boos, W. Kruppa, B. R. Bennett, D. Park, S. W. Kirchoefer, R. Bass, and H. B. Dietrich, *IEEE Trans. Electron. Devices* **45**, 1869 (1998).
- <sup>6</sup>D. H. Chow, H. L. Dunlap, W. Williamson III, S. Enquist, B. K. Gilbert, S. Subramaniam, P.-M. Lei, and G. H. Bernstein, *IEEE Electron Device Lett.* **17**, 69 (1996).
- <sup>7</sup>Q. Du, J. Alperin, and W. I. Wang, *Appl. Phys. Lett.* **67**, 2218 (1995).
- <sup>8</sup>M. Yano, H. Yokose, Y. Iwai, and M. Inoue, *J. Cryst. Growth* **111**, 609 (1991).
- <sup>9</sup>O. Brandt, E. Tournie, L. Tapfer, and K. Ploog, *J. Cryst. Growth* **127**, 503 (1993); M. Nouaoura, F. W. O. Da Silva, N. Bertru, M. Rouanet, A. Tahraouri, W. Oueini, J. Bonnet, and L. Lassabaterre, *ibid.* **172**, 37 (1997).
- <sup>10</sup>J. Schmidt, J. Wagner, F. Fuchs, N. Herres, P. Koidl, and J. D. Ralston, *J. Cryst. Growth* **150**, 858 (1995).
- <sup>11</sup>M. Yano, T. Utatsu, Y. Iwai, and M. Inoue, *J. Cryst. Growth* **150**, 868 (1995).
- <sup>12</sup>B. V. Shanabrook, J. R. Waterman, J. L. Davis, and R. J. Wagner, *Appl. Phys. Lett.* **61**, 2338 (1992).
- <sup>13</sup>B. V. Shanabrook, B. R. Bennett, and R. J. Wagner, *Phys. Rev. B* **48**, 17172 (1993).
- <sup>14</sup>B. V. Shanabrook and B. R. Bennett, *Phys. Rev. B* **50**, 1695 (1994).
- <sup>15</sup>B. V. Shanabrook and B. R. Bennett, *Proceedings of the 22nd International Conference Phys. Semic., Banff, Canada, 1995*, p. 955.
- <sup>16</sup>R. Perez-Alvarez and C. Trallero-Giner, *Phys. Scr.* **56**, 407 (1997).
- <sup>17</sup>M. E. Twigg, B. R. Bennett, P. M. Thibado, B. V. Shanabrook, and L. J. Whitman, *Philos. Mag. A* **77**, 7 (1998).
- <sup>18</sup>A. Ourmazd, D. W. Taylor, J. Cunningham, and C. W. Tu, *Phys. Rev. Lett.* **62**, 933 (1989).
- <sup>19</sup>S. Thoma and H. Cerva, *Ultramicroscopy* **38**, 265 (1991).
- <sup>20</sup>M. W. Wang, D. A. Collins, T. C. McGill, and R. W. Grant, *J. Vac. Sci. Technol. B* **11**, 1418 (1993).
- <sup>21</sup>D. A. Collins, M. W. Wang, R. W. Grant, and T. C. McGill, *J. Vac. Sci. Technol. B* **12**, 1125 (1994).
- <sup>22</sup>P. V. Neklyudov, S. V. Ivanov, B. Ya. Mel'tser, and P. S. Kop'ev, *Semiconductors* **31**, 1067 (1997).
- <sup>23</sup>B. R. Bennett, B. V. Shanabrook, R. J. Wagner, J. L. Davis, and J. R. Waterman, *Appl. Phys. Lett.* **63**, 949 (1993).
- <sup>24</sup>G. Tuttle, H. Kroemer, and J. H. English, *J. Appl. Phys.* **67**, 3032 (1990).
- <sup>25</sup>B. R. Bennett, B. V. Shanabrook, and E. R. Glaser, *Appl. Phys. Lett.* **65**, 598 (1994).
- <sup>26</sup>B. R. Bennett, B. V. Shanabrook, E. R. Glaser, and R. J. Wagner, *Mater. Res. Soc. Symp. Proc.* **340**, 253 (1994).
- <sup>27</sup>D. H. Chow, R. H. Miles, J. R. Soderstrom, and T. C. McGill, *Appl. Phys. Lett.* **56**, 1418 (1990).
- <sup>28</sup>J. L. Davis, R. J. Wagner, J. R. Waterman, B. V. Shanabrook, and J. O. Omaggio, *J. Vac. Sci. Technol. B* **11**, 861 (1993).
- <sup>29</sup>F. Fuchs, U. Weimer, E. Ahlswede, W. Pletschen, J. Schmitz, and M. Walther, *Proc. SPIE* **3287**, 14 (1998).
- <sup>30</sup>M. J. Yang, W. J. Moore, B. R. Bennett, and B. V. Shanabrook, *Electron. Lett.* **34**, 270 (1998).